Electrical microstimulation evokes saccades in posterior parietal cortex of common marmosets

Maryam Ghahremani [1,4], Kevin D. Johnston [1,2,3], Liya Ma[4], Lauren Schaeffer [4], Stefan Everling[1,2,3,4]

[1] Graduate Program in Neuroscience, The University of Western Ontario, London, Ontario, Canada; [2] Department of Physiology and Pharmacology, The University of Western Ontario, London, Ontario, Canada; [3] Brain and Mind Institute, The University of Western Ontario, London, Ontario, Canada; [4] Robarts Research Institute, The University of Western Ontario, London, Ontario, Canada.

Author Contributions

MG performed experiments, analysed data, prepared the figures, and wrote the first draft of the manuscript. KJ designed experiments, performed experiments, and edited the manuscript. LM helped with the surgery, performed perfusion and brain extraction and edited the manuscript, LS performed experiments and edited the manuscript. SE designed experiments, performed surgeries, edited the manuscript, and approved the final version of the manuscript.

Running head title

Microstimulation of marmoset posterior parietal cortex

Corresponding author

Stefan Everling, severlin@uwo.ca, Centre for Functional and Metabolic Mapping, Robarts Research Institute, 1151 Richmond Street North, London, Ontario, N6A 5B7, Canada, Phone: (519) 663 5777 x 24359, Fax: (519) 663 3193.

Keywords: common marmoset; posterior parietal cortex; area LIP; saccade; microstimulation

Abstract

The common marmoset (*Callithrix jacchus*) is a small-bodied New World primate, increasing in prominence as a model animal for neuroscience research. The lissencephalic cortex of this primate species provides substantial advantages for the application of electrophysiological techniques such as high-density and laminar recordings, which have the capacity to advance our understanding of local and laminar cortical circuits and their roles in cognitive and motor functions. This is particularly the case with respect to the oculomotor system, as critical cortical areas of this network such as the frontal eye fields (FEF) and lateral intraparietal area (LIP) lie deep within sulci in macaques. Studies of cytoarchitecture and connectivity have established putative homologies between cortical oculomotor fields in marmoset and macaque, but physiological investigations of these areas, particularly in awake marmosets, have yet to be carried out. Here, we addressed this gap by probing the function of posterior parietal cortex (PPC) of the common marmoset using electrical microstimulation. We implanted two animals with 32-channel Utah arrays at the location of the putative area LIP and applied microstimulation while they viewed a video display and made untrained eye movements. Similar to previous studies in macaques, stimulation evoked fixed-vector and goal-directed saccades, staircase saccades, and eye blinks. These data demonstrate that area LIP of the marmoset plays a role in the regulation of eye movements, provide additional evidence that this area is homologous with that of the macaque, and further establish the marmoset as valuable model for neurophysiological investigations of oculomotor and cognitive control.

Introduction

The common marmoset (*Callithrix jacchus*) has recently gained considerable attention as a model for biomedical research in general (Mansfield, 2003) and neuroscience research in particular (Belmonte et al., 2015; Mitchell & Leopold, 2015; Miller et al., 2016; French, 2019). Accordingly, considerable effort has been directed toward mapping the marmoset brain (Okano & Mitra, 2015), and establishing homologies between cortical areas in this species and the macaque (Paxinos, 2012; Solomon & Rosa, 2014; Bakola et al., 2015), which to date has been the most commonly used primate model. The marmoset model also holds substantial promise for the study of oculomotor control. Marmosets are highly visual, foveate animals that make both saccadic and smooth pursuit eye movements (Mitchell et al., 2014; Mitchell et al., 2015), and possess a lissencephalic cortex well-suited to laminar and high-density recordings (Mitchell & Leopold, 2015). In comparison to the macaque model, however, our knowledge of marmoset oculomotor areas is currently at an emergent stage, and it remains to establish the anatomical and physiological correspondences between cortical eye fields in the two species.

The cortical and subcortical circuitry controlling saccadic eye movements is perhaps the most thoroughly understood sensorimotor system in the primate brain (Munoz et al., 2000; Schiller & Tehovnik, 2001). In the macaque, these areas include the frontal eye fields (FEF) (Bruce & Goldberg, 1985) and lateral intraparietal area (LIP) (Andersen et al., 1987), both of which send direct projections to the midbrain superior colliculus (SC) (Selemon & Goldman-Rakic, 1988), an area critical for saccade generation. These cortical areas are buried deep within sulci in this species which highlights the advantages of marmosets with their smooth cortex. Here, we investigated the oculomotor properties of the marmoset posterior parietal cortex. In this species, the picture with respect to the parcellation and homology of the marmoset posterior parietal cortex (PPC) is thus far considerably less clear than is understood in the macaque. Using cyto and myeloarchitecture, Rosa et al. (2009) separated the marmoset PPC into two main subdivisions, PPd (dorsal posterior parietal) and PPv (ventral posterior parietal). Based on the similar pattern of myelination within marmoset PPd and macaque parietal cortex (Blatt et al., 1990), and the presence of large layer V pyramidal neurons, they proposed that this subregion contained the likely homologue of macaque LIP. Subsequent anatomical (Collins et al., 2005; Reser et al, 2013) and resting-state fMRI (Ghahremani et al., 2017) investigations have

supported this view as they have shown triangulated connectivity of this area with the putative FEF and SC. As has been previously noted by other authors however (Solomon & Rosa, 2014), the identification of area LIP requires confirmation with electrophysiological techniques in awake animals to establish common functional properties.

Intracortical microstimulation has long been used as a tool to characterize the properties of brain areas by activating neuronal populations (see for review Clark et al., 2011; Tehovnik et al., 2006). Microstimulation of PPC in the awake behaving macaque has been shown to evoke body movements, eye blinks, and both saccadic and smooth eye movements (Fleming & Crosby, 1955; Keating et al., 1983; Shibutani et al., 1984; Kurylo & Skavenski, 1991). Thier & Andersen (1998) subsequently found that the region from which saccades could be evoked was restricted to area LIP within the lateral bank of the intraparietal sulcus, from which they observed both fixed-vector saccades, for which amplitude and direction were invariant with respect to initial eye position, and convergent or goal-directed saccades which tended to drive the eyes to a fixed goal location in space. To date, no studies have investigated the oculomotor properties of the cytoarchitectonically defined region LIP in the common marmoset. Here, we applied for the first time electrical microstimulation to the PPC of awake behaving marmosets and monitored eye position while the animals were allowed to make unrestricted eye movements. To ensure maximal coverage of the cortical area, we implanted 32 channel Utah arrays in area LIP of two marmosets and applied stimulation trains of varying currents. Similar to previous findings in macaque monkeys, we observed eye blinks as well as both fixed-vector and convergent saccades. These data suggest that area LIP of marmoset plays a similar role to that of the macaque in the modulation of eye movements.

Methods

Subjects

Two male common marmoset (*Callithrix jacchus*) monkeys weighing 440 g and 451g each, and aged 2.5 and 4 years were subjects in the experiment. All experimental procedures conducted were in accordance with the Canadian Council of Animal Care policy on the care and use of

laboratory animals and an ethics protocol approved by the Animal Care Committee of the University of Western Ontario. The health and welfare of animals was under the close supervision of university veterinarians.

Details of surgical procedures and training methods involved in preparation of the animals for awake behaving experiments have been previously described (Johnston et al, 2018). Briefly, each animal was acclimated to restraint within a custom-designed primate chair and subsequently underwent an aseptic surgical procedure in which a combination recording chamber/head holder was attached to the skull using dental resin and adhesive (Bisco All-Bond, Bisco Dental Products, Richmond, BC, Canada). This allowed restraint of the head within a custom-designed stereotaxic frame during experimental sessions.

Following subsequent additional training to acclimate the animals to head restraint, a second aseptic surgery was carried out in which a 32 channel Utah array (Blackrock Microsystems, Salt Lake City, UT, USA) was inserted into the posterior parietal cortex (PPC) of each monkey. Electrodes within these arrays were 1mm in length and had an inter-electrode spacing of 400 μm. During this surgery, a microdrill was used to open 4mm burr holes in the skull to allow access to PPC at locations based upon the stereotaxic coordinates of area LIP (1.4 mm anterior, 6 mm lateral) (Paxinos, 2012) which corresponds to the location of a posterior parietal region previously shown to have strong resting-state connectivity with the midbrain superior colliculus (SC) (Ghahremani et al., 2017). We additionally confirmed these locations visually by noting the location of a small blood vessel corresponding to the location of a shallow sulcus believed to be homologous to the intraparietal sulcus of other primate species. Arrays were manually inserted such that the width of the array straddled the sulcus and the array length covered as much of the sulcus length as possible. Following array insertion, the array wires and connector were fixed in place within the recording chamber using dental adhesive, and the array and remaining exposed cortical surface within the burr hole were covered with medical-grade silicone elastomer adhesive (World Precision Instruments, Sarasota, FLA, USA). A screw-hole was drilled into the skull posterior to the location of the implanted array to place the ground screw. The ground wire of the array was then tightly wound around the base of the screw to ensure good electrical connection. Any remaining exposed wire was then covered with additional protective layers of dental adhesive as required. After full curing of the adhesive, a removable protective cap was fixed in place on the recording chamber.

Microstimulation Protocol

Prior to applying microstimulation, we first verified that individual sites in the microelectrode array were within cortex by monitoring for extracellular neural activity using the Open Ephys acquisition board (http://www.open-ephys.org) and digital headstages (Intan Technologies, Los Angeles, CA, USA). For both animals, spike activity began about 2 weeks following array implant surgery. Microstimulation pulses were delivered using the Intan RHS2000 Stimulation/Recording Controller system and digital stimulation/recording headstages (Intan Technologies, Los Angeles, CA, USA). Stimulation trains consisted of 0.3ms biphasic current pulses delivered at 300 Hz for a duration of 100-300ms, at current amplitudes varying between 40 and 240 μA. For those sites at which saccades were evoked, we additionally determined the threshold current, defined as the minimum current at which saccades could be evoked on 50% of stimulation applications. In sessions investigating whether saccades could be evoked at individual array sites, eye movements were uncontrolled and microstimulation trains were triggered manually by the experimenter. In those on which we investigated effects of initial eye position on saccade direction and amplitude, stimulation trains were triggered by behavior control software based on fixation location and duration criteria (see Eye Movement Recording, below).

Eye Movement Recording

Animals were seated in a primate chair that was integrated with a custom designed stereotaxic frame for head restraint and eye movement recording. The chair/frame system was mounted on a table within a sound-attenuating chamber (Crist Instruments Co., Hagerstown, MD, USA). Their heads were restrained and a liquid spout placed at their mouth for reward delivery. Rewards consisted of acacia gum and were delivered via infusion pump (Model NE-510, New Era Pump Systems, Inc., Farmingdale, New York, USA). Eye positions were monitored via high-speed (1000 Hz) infrared video oculography which monocularly tracked pupil location (EyeLink 1000, SR Research, Ottawa, ON, Canada), and recorded together with microstimulation parameters using the Intan Simulation/Recording controller. Eye position was calibrated in each session by requiring marmosets to fixate on images of marmoset faces presented at several predetermined locations, in order to receive a liquid reward. All stimuli were presented on a CRT monitor

(ViewSonic Optiquest Q115, 76 Hz non-interlaced, 1600 x 1280 resolution) at a viewing distance of 42cm. Stimulus presentation and reward delivery were carried out under computer control using the CORTEX real-time operating system (NIMH, Bethesda, MD, USA).

In the initial series of microstimulation sessions, animals freely viewed video images on the CRT monitor while we manually applied stimulation trains at single array sites and monitored the animals' horizontal and vertical eye positions to determine whether saccades could be evoked at a given site. For those sites at which saccades could be reliably evoked, we carried out stimulation current series to determine saccade thresholds. Rewards were given manually by the experimenters to maintain the animals' level of alertness throughout the session but were not contingent on any oculomotor behavior. To further investigate effects of initial eye position on saccade directions and amplitudes, in a subsequent series of sessions we revisited many of the sites at which saccades could be evoked and applied stimulation under computer control while the animal's initial eye positions were at each of a set of predetermined locations. In these sessions, animals freely viewed the same video images and stimulation trains were triggered by the CORTEX real-time operating system when their eye positions were maintained within 5 x 5 degree electronic windows centred on one of a series of predetermined locations for a period of 100 ms. Locations were at an eccentricity of 7 degrees at the upper left, lower left, upper right, and lower right quadrants of the display monitor, or at the monitor centre.

Confirming Array Location

Ex vivo MRI for marmoset B and in vivo micro-CT scan for marmoset W were conducted to confirm the positioning of the array with respect to local landmarks and the putative area LIP. As marmoset W was involved in further data experiments, a micro-CT scan was carried out to determine the array location brain of this animal.

Ex vivo MRI scan

Marmoset B was sacrificed at the end of the data acquisition process to prepare the brain for ex vivo MRI scan. The animal was deeply anesthetized with 20 mg/kg of ketamine plus 0.025

mg/kg Medetomidine and 5% isoflurane in 1.4-2% oxygen to reach beyond the surgical plane (i.e. no response to toe pinching or cornea touching). It was then transcardially perfused with 200 ml of phosphate buffered saline, followed by 200 ml of 10% buffered formalin. The brain was then extracted and stored in 10% buffered formalin for more than a week prior to performing the ex vivo scan. On the day of the scan, the brain was transferred to another container for imaging and immersed in a fluorine-based lubricant, Christo-lube (Lubrication Technology, Inc), to improve homogeneity and avoid susceptibility artifacts at the boundaries. The ex vivo image was then acquired using a 9.4T, 31 cm horizontal bore magnet (Varian/Agilent) and Bruker BioSpec Avance III console with the software package Paravision-6 (Bruker BioSpin) and a custom-built 15-cm-diameter gradient coil with 400 mT/m maximum gradient strength (xMR, London, Ontario, Canada; Peterson et al., 2018). An ex vivo T2-weighted image was acquired with the following scanning parameters: repetition time (TR) = 5s, echo time (TE) = 45 ms, field of view (FOV) = 40 × 32, image size = 160 × 128, slice thickness = 0.5 mm.

To identify the location of the previously implanted array, the resulting T2-weighted image was registered to the NIH marmoset brain atlas (Liu et al., 2018) using the registration packages of the FSL software (fMRI Software Library: http://www.fmrib.ox.ac.uk). Upon visual examination of the image, an indentation of comparable size to the array (3 mm) was identified on the surface of the cortex within the PPC that represented the array location. The location of this region of interest was interpolated on the cortical surface to create a mask across this indentation. The mask was then projected on to the surface space in CARET toolbox (Van Essen et al., 2001), using a surface-based version of the NIH volume template that was kindly provided by the authors of the NIH marmoset brain template (Liu et al., 2018). The array mask was then compared to the area LIP as defined by the parcellated regions of the NIH template, that was also projected on CARET surface space.

In vivo micro-CT scan

Marmoset W was imaged on a live-animal micro-CT scanner (eXplore Locus Ultra, GR Healthcare Biosciences, London, ON) to identify the location of the array on the brain. Prior to the scan, the animal was anesthetized with 15mg/kg Ketamine mixed with 0.025mg/kg Medetomidine. It was then placed on the CT bed in supine position with arms along its sides. X-

ray tube potential of 120 kV and tube current of 20 mA were used for the scan, with the data acquired at 0.5º angular increment over 360º, resulting in 1000 views. The resulting CT images were then reconstructed into 3D with isotropic voxel size of 0.154 mm. Heart rate and SpO2 were monitored throughout the session. At the end of the scan, the injectable anesthetic was reversed with an IM injection of 0.025mg/kg Ceptor.

To find the location of the array with respect to the NIH template, the acquired CT image was brain extracted while including the trace of the array across the boundary of the cortex. The brain extracted image was then registered to the NIH marmoset brain atlas (Liu et al., 2018) using the FSL software (fMRI Software Library: http://www.fmrib.ox.ac.uk). Similar to the ex vivo MRI data, an ROI mask was created over the traces of the array across the surface of the cortex to represent the location of the array. This mask was projected on the surface space using CARET.

Data Analysis

All eye movement analyses were carried out using custom-written codes in MATLAB (The Mathworks, Natick, MA). Horizontal and vertical eye traces were low-pass filtered at 30 Hz and horizontal and then aligned with the stimulation onset to detect changes in eye movements following the stimulation pulse. We only considered changes in eye position that were greater than 2º and fell within a window of 200ms from the onset of microstimulation. Saccades were detected based on first order derivative, corresponding to the velocity of eye movements. The start of a saccade was defined by the first time point in which the speed of the eye movement reached 30 º/s and the first time point at which the speed went back to zero marked the end point of saccade. All saccades were normalized to the baseline by subtracting the mean of the eye position within a 50ms window before the onset of stimulation. Saccade amplitudes were defined based on the start and endpoints of saccades, as determined by the velocity criteria. The obtained values per trial were then averaged across all saccadic trials for each site of the microelectrode array. Saccade latency was defined as the time from the onset of microstimulation to the onset of the saccade. The duration of saccades was calculated based on the difference between the time point of the start and end of saccades. The same procedures were employed in those sessions in which we investigated

the effect of initial eye position, except that in this case saccades were not normalized to baseline. To quantify the effect of initial eye position on microstimulation-evoked saccades, we applied the linear regression modeling technique proposed by Russo and Bruce (1993). For every site of interest, the size of the saccades defined as the difference of saccade offset and onset, was plotted versus all different initial eye positions to produce scatter plots for horizontal and vertical saccade components, separately. A line of regression was fit into each scatter plot, the slope of which represented the effect of initial eye position on elicited saccades. A value that was closer to zero indicated that the elicited saccades had mostly unchanged trajectories, independent of the initial eye position. This is referred to as fixed-vector saccades. A value close to 1 or -1 implied that the elicited saccades changed trajectory depending on the initial eye position and converged towards a common orbital position irrespective of the initial eye position.

Results

Confirming the location of the array

The results of the ex vivo MRI for marmoset B and in vivo micro-CT scan for marmoset W are depicted in figure 1. The figure on the left displays the location of the array for both marmoset B (red patch) and marmoset W (blue patch) registered on the surface space of the left hemisphere of the marmoset brain using CARET surface registration toolbox, with the cytoarchitectonic boundaries overlaid in white. The figure on the right displays the location of the arrays in more detail, by enlarging the area enclosed within the blue box as shown on the left figure, with all the overlapping and neighboring areas labelled according to the NIH brain parcellation map (Liu et al., 2018). The purple patch in these figures demonstrates the overlapping area between the arrays from both animals. As can be observed, the array location mostly fell within the boundaries of area LIP, while covering parts of areas MIP and VIP in both animals.

Oculomotor Effects of LIP Microstimulation

In both animals, microstimulation of area LIP evoked saccades and eye blinks at multiple sites of the implanted array. For Marmoset B, we observed saccades at 21/32 sites, and eye blinks at 2/32 sites. For Marmoset W, we observed saccades at 23/32 sites, and eye blinks at 9/32 sites. Figure 2A depicts this pattern of observations across all sites of the array for both animals. As can be seen from the figure, saccades were evoked at many array sites, with the exception of the most anterior sites, from which we obtained either blinks (Marmosets W and B), or no response (Marmoset B). For most sites at which microstimulation evoked saccades, we carried out current series to determine saccade thresholds, which we defined as the current at which saccades could be evoked on 50% of trials. Thresholds ranged from 40 to 240 μA. The topography of saccade thresholds is depicted in figure 2B. We generally noted higher thresholds in Marmoset B, which was most likely attributable to the depth of the electrodes within cortex for this animal. We did not observe a clear pattern of threshold topography in either animal.

An example of a microstimulation-evoked saccade is presented in figure 3 from a representative site in Marmoset W (marked in grey in the on the bottom right figure). Here, microstimulation currents of varying amplitudes (75, 100, 200 μA) elicited contralateral saccades with an upward vertical component (fig. 3A). In general, we noted that the probability of evoking a saccade at a responsive site increased as a function of stimulation current (fig. 3B).

Saccade Latency and Duration

Saccade onset latency was defined as the time from the onset of the microstimulation pulse to saccade onset. Latency values were averaged across all trials of all saccade-eliciting sites for both animals and plotted as a function of the stimulation current, ranging from 50 to 240 μA (fig. 4A). Onset latencies declined as a function of the stimulation current. Mean latencies ranged from 64 ms at 200-250 μA to 87 ms when currents were in the range of 50-100 μA. Error bars were calculated based on the standard error from the mean.

Saccade duration was defined as the time from saccade onset to the end of saccade. This parameter was similarly averaged across all trials of all saccade-eliciting sites of the array for both monkeys and plotted against stimulation current amplitude. As demonstrated in figure 4B, saccade

duration was 20 ms on average and there was no significant difference in saccade duration across different stimulation current amplitudes. Error bars were calculated based on the standard error from the mean.

Staircase saccades

At some sites within the array, prolonged (300 ms) stimulation evoked staircase saccades, separated by intervals of variable duration (80 to 140 ms). There were four such sites identified in marmoset W that exactly overlapped with sites from which fixed-vector saccades were elicited. There was only one site with staircase saccade identified in marmoset B. Two examples of such staircase saccades in marmoset W are shown in figure 5 from two individual sites that were stimulated at current amplitudes of 150 and 225 μA, respectively. The amplitude of the saccades within the staircase sequence decreased in some cases (fig. 5 left) and was less variable in other cases (fig. 5 right), while the direction of the saccades within the staircase remained the same in most cases observed.

Saccade Direction and Amplitude

Saccade direction and amplitude were calculated based on the slope and amplitude of horizontal and vertical eye traces, between the start point and end point of saccades for each saccadic site of the array. These parameters were represented as arrows with their associated direction and amplitude. To determine the general topography of saccade directions and amplitudes, all saccades evoked at each specific site were averaged together, resulting in an average saccade vector for that site. This procedure was repeated for all saccadic sites of the array for each animal and the resulting saccade vectors were mapped onto their associated location within the array (figure 6A). The result demonstrated that the majority of microstimulation-evoked saccades exhibited a prominent upward bias, contralateral to the site of stimulation, in both animals across most sites of the array (figure 6A). There were few sites in Marmoset B that exhibited downward saccades. However, the horizontal component of the evoked saccades was always contralateral to the site of stimulation. In terms of the saccade amplitude, varying amplitudes were

observed across array sites in both animals with more centrally located sites having larger amplitudes in general.

Effects of initial eye position

Based on the previous literature on macaque LIP, it has been reported that one of the factors influencing the direction or amplitude of saccades induced by LIP microstimulation is the initial position of the eye at the time of microstimulation (Shibutani et al., 1984; Kurylo and Skavenski, 1991; Thier & Andersen, 1996; Their & Andersen, 1998). To investigate this in the marmoset PPC, in a subset of sessions and sites we applied microstimulation whenever the animal's eye position fell within one of 7 predefined zones. Next, we applied regression analysis to each of these sites for horizontal and vertical saccade components individually, to examine the impact of initial eye position on the convergence of the elicited saccades. The slope of the regression line was calculated and used as an index to indicate the level of the impact (Russo and Bruce, 1993). Out of the 10 saccadic sites investigated, three sites exhibited saccades for which amplitude and direction were modified such that eye position was driven to converge on a common location, from any starting position across the display. An example of such sites is shown in figure 7A (right) from a representative site of the array in marmoset W with its corresponding regression analysis plots (7B, right). The location of these sites is marked within the array grid as displayed on the top right of each plot. The slope of the regression line for horizontal saccade component (K_h, blue) in this site was 0.24 and for vertical component (K_v, red) was 0.65. The preferred "goal zone" was generally located in the contralateral upper visual field as demonstrated in the representative example of figure 7A (right). Most of the remaining sites exhibited fixed-vector saccades that maintained nearly the same amplitude and direction irrespective of the starting position of the eye at the onset of microstimulation. A representative site that elicited such fixed-vector saccades in marmoset W is shown in figure 7A (left) with its corresponding regression analysis plot (7B, left). Here, the slope of the regression line for horizontal saccade component (K_h, blue) in this site was 0.02 and for vertical component (K_v, red) was -0.03, which were much closer to 0 compared to the representative site for the goal-directed saccade (fig. 7A, right). There were few sites that exhibited saccades that did not exactly belong to either category. All evoked saccades (vector or goal-directed) however exhibited an upward bias, contralateral to the site of stimulation. Figure 8

displays the slopes of the regression line for both horizontal (left, K_h) and vertical (right, K_v) saccade components plotted as bar graphs for all the 10 sites in which the effect of initial eye position was investigated. The location of these sites is marked on the array grid as shown on the top left. For the three sites that seemed to elicit goal-directed saccades, K_h was in the range of 0.14 to 0.25, which was comparable to other sites (fig. 8, left). However, in these three sites K_v varied from 0.5 to 0.6 which was higher than the slope of the vertical saccade components of all the other sites (fig. 8, right). In the case of remaining sites, the slope of the regression line for horizontal saccade components (K_h) ranged from 0.01 to 0.2 and for vertical saccade components (K_v) ranged from -0.1 to 0.37.

Discussion

Here, we applied intracortical microstimulation to a subregion of the PPC, area LIP, to investigate the oculomotor properties of this area in common marmosets. We observed a suite of oculomotor responses including fixed-vector saccades, goal-directed craniocentric saccades, and staircases of saccades. In all cases, saccades were directed toward the hemifield contralateral to the site of stimulation, and predominantly toward the upper visual field. In some cases, we also observed eye blinks. These findings are consistent with previous electrical stimulation studies of PPC in the macaque model (Shibutani et al., 1984; Kurylo & Skavenski, 1991; Thier & Andersen, 19967; Thier & Andersen, 1998), and support the view that LIP of the marmoset has similar oculomotor properties as that of macaque.

A consistent finding of microstimulation experiments in macaque LIP is the presence of two broad classes of saccades. So-called “modified vector” or retinotopic saccades with relatively consistent directions and amplitudes regardless of the initial position of the eyes, and “goal-directed” or craniocentric saccades, the amplitudes and directions of which vary with initial eye position such that they tend to be driven toward a particular goal location (Kurylo & Skavenski, 1991; Thier & Andersen, 1996; Thier & Andersen, 1998). Sites at which these saccade types can be evoked have a topographic distribution, such that vector saccades are evoked at more caudal sites, while goal-directed saccades are confined to a small rostral region in the floor of the of the intraparietal sulcus and extending into the medial bank, termed the “intercalated zone” (Thier & Andersen, 1996; Thier & Andersen, 1998). We similarly observed

both classes of saccades following microstimulation of marmoset area LIP. We found, however that goal-directed saccades were rare, and were not restricted to a specific cluster of sites but rather were interdigitated with sites at which vector saccades were evoked. One possible explanation for the relative lack of goal-directed sites we observed is the limited oculomotor range of the marmoset. In some cases, the goal-directed saccades evoked from macaque intraparietal sulcus drove the eyes to a goal location beyond the range of ocular motility (Kurylo & Skavenski, 1991; Thier & Andersen, 1996). In marmosets, the oculomotor range is limited to approximately 12 degrees, which is considerably less than the approximately 30 degree eccentric range of the macaque (Tomlinson & Bahra, 1986; Heiney & Blazquez, 2011). Marmosets also rely more on movements of the head to shift gaze (Mitcthell et al., 2014). It thus seems possible that we failed to observe convergent eye movements due to the face that we were able to analyse only the initial few degrees of the eye trajectories of gaze shifts converging well outside the oculomotor range, and thus underestimated the number of sites at which goal-directed saccades could be evoked. Alternatively, such sites may simply be more rare and widely distributed in marmoset PPC. Consistent with this idea, we found that eye blinks but not goal-directed saccades could be evoked the most rostral sites in both animals. In contrast, in macaque both eye blinks and goal-directed saccades could both be evoked from the intercalated zone in the rostral portion of area LIP (Thier & Andersen, 1996; Thier & Andersen, 1998). Whether this difference in co-localization of responses represents a real phylogenetic difference in modularity of PPC organization (Krubitzer, 1995) between these primate species remains to be definitively determined, though we noted also a continuity of sites from which saccades could be evoked in marmosets, contrasting with the typical "fractured" distribution of sites in macaque LIP, in which sites from which saccades can be evoked are organized in clusters separated by non-responsive bands of cortex (Thier & Andersen, 1996).

In contrast to differences in the distribution of goal-directed saccades, we observed a similar topography of saccade directions in marmoset area LIP to previous findings in macaque. The directions of evoked saccades were toward the contralateral hemifield in all cases in both animals, and in the vast majority of cases these saccades had an upward component. A small number of sites with a downward component were observed in marmoset B, either at the most rostral or caudal sites. Amplitudes of evoked saccades varied from 3 to 12 degrees. In neither animal did we observe a clear topographic organization of either of these saccade parameters. In

macaque LIP, microstimulation has been shown to evoke contralateral saccades with a strong upward bias and no clear organization with respect to direction or amplitude (Kurylo & Skavenski, 1991; Thier & Andersen 1996; Thier & Andersen, 1998).

Previous studies investigating the effects of intracortical microstimulation on motor responses in marmosets have reported that the thresholds for evoking movements is greater in this species than macaques (Burman et al., 2008), possibly due to the smaller soma size and hence decreased electrical excitability of pyramidal neurons in marmosets (Nudo et al., 1995). We systematically obtained thresholds at most PPC sites from which we were able to evoke eye movements, and found that thresholds varied from 40 – 240 μA, values similar to those observed in previous studies of macaque PPC which in the literature have typically ranged from 25- 200 μA (Shibutani et al., 1984; Kurylo & Skavenski, 1991; Their & Andersen, 1998). This similarity is perhaps surprising as the Utah arrays we used here did not allow us to optimize the cortical depths at which stimulation was applied by moving individual electrodes. We did note however that the latencies of evoked saccades were greater following stimulation of marmoset LIP than most prior studies in macaque. We obtained latencies of 64-87ms, in comparison to the mean latencies of 30 and 50 ms found by Thier & Andersen (1998), and Shibutani et al. (1984), respectively. Whether this represents a true species difference in the role of area LIP in the control of saccades or is simply a reflection of reduced soma and axon sizes in the smaller New World marmoset remains to be determined. Studies investigating the response properties of single LIP neurons during saccades, as well as studies in the marmoset FEF should prove illuminating in this regard.

Many previous studies applying microstimulation to macaque PPC have observed evoked movements of not only the eyes, but also the pinnae, face, arms, and shoulders (Fleming & Crosby, 1955; Shibutani et al., 1984; Kurylo & Skavenski, 1991; Thier & Andersen, 1998; Cooke et al., 2003). Although we monitored the animals here for these effects, we did not observe any such movements following stimulation. This may be at least partially explained by the size and locations of the implanted microelectrode arrays. Each array was implanted on the basis of resting-state fMRI and the local sulcal landmark such that it was placed roughly straddling the sulcus in mediolateral extent and centred with respect to the sulcus in rostrocaudal extent, in order to cover as much of the putative area LIP as possible. In marmoset, area LIP extends approximately 3.5 – 4mm rostro-caudally, and 2 mm medio-laterally. The dimensions of

our arrays were 3 x 3 mm, and thus may have been located predominantly within the borders of area LIP, at least rostrocaudally. Thier and Andersen (1998), found that within macaque area LIP itself, movements other than those of the eyes were evoked only in the intercalated zone from which goal-directed saccades could be evoked, at the most rostral extent of LIP. No movements other than those of the eyes were evoked at the more caudal sites from which fixed-vector saccades were evoked. Since we found that fixed-vector saccades were evoked at the majority of sites in both animals, it seems reasonable to suggest that most of our stimulation sites were restricted to the region specific to fixed-vector eye movements, and simply did not reach cortex from which non-eye movements could be evoked. On the other hand, we did observe eye blinks at a few stimulation sites in both animals that possibly covered parts of area VIP, consistent with observations in area VIP in macaques, a region from which defensive movements of the arms and face can also be evoked (Cook et al., 2003). Future work using larger arrays covering a greater extent of PPC or greater cortical sampling by other means would definitely address this discrepancy in findings.

The recent increase in popularity of the marmoset model has been paralleled by anatomical studies aiming to establish homologies between cortical areas of the marmoset and rhesus macaques, which historically have been the most commonly used primate model in neuroscience research (Solomon & Rosa, 2014). In a similar vein, behavioural work has demonstrated that marmosets display many similarities with macaques with respect to their visual and oculomotor behaviour (Mitchell et al., 2014; Johnston et al., 2018; Johnston et al. 2019). To date however, few studies have investigated the properties of cortical areas involved in oculomotor control in awake behaving marmosets, which is a critical step in determining the function of these areas and relating them to macaques and ultimately human brain function. It has been proposed that homology between cortical fields can be established on the basis of three primary criteria: cytoarchitecture, connectivity, and neural response properties (Kaas, 1987; Krubitzer, 1995). With respect to area LIP, corresponding aspects of cytoarchitecture between macaques and marmosets such as dense myelination and the presence of large layer V pyramidal neurons have been established (Rosa et al., 2009; Bock et al, 2009). Similarly, area LIP shares a common pattern of connectivity across species. This area was originally defined in macaques as a subregion within the intraparietal sulcus with extensive interconnections to the FEF and SC (Andersen et al., 1985). Such connectivity has been established in marmoset on the basis of

anatomical (Reser et al., 2013; Collins et al., 2005) and resting-state fMRI (Ghahremani et al., 2017). Our data here suggest that the functional properties of LIP in both species are also similar. Although we noted some differences in the proportions and distributions of the two types of microstimulation-evoked saccades in the two species, we found that saccades could be evoked at similar currents, at marginally longer latencies, and with a similar direction bias toward the upper contralateral visual field as previous studies in macaques. Although single neuron recordings in area LIP of marmosets trained to perform oculomotor tasks are needed to definitively establish correspondence in neuronal response properties, taken together, these three existing lines of convergent evidence provide compelling support for the notion that marmoset LIP is homologous with that of macaque monkeys, and establish further the marmoset as a promising new model for the study of oculomotor and cognitive control.

Acknowledgements

We thank N. Hague, C. Vander Tuin, W. Froese, and K. Faubert for surgical assistance and care of the experimental animals.

Figure legends

Figure 1. The results of the ex vivo MRI for marmoset B and in vivo micro-CT scan for marmoset W to identify the positioning of the array. The figure on the left displays the location of the array for both marmoset B (red patch) and marmoset W (blue patch) registered on the surface space of the left hemisphere of the marmoset brain, with cortical boundaries overlaid in white. The figure on the right displays the location of the arrays in more details, by zooming into the area enclosed within the blue box as shown on the left figure, with all the overlapping and neighboring areas labelled according to the NIH brain parcellation map (Lui, 2018). The purple patch in these figures demonstrates the overlapping area between the arrays from both animals. LIP: lateral intraparietal area, MIP: medial intraparietal area, VIP: ventral intraparietal area, AIP: anterior intraparietal area, PE: parietal area PE, PEC: caudal part of parietal area PE, PG: parietal area PG, OPt: occipito-parietal transitional area, V6A: visual area 6A, V3A: visual area 3A.

Figure 2. (A) Mapping the results of electrical microstimulation on individual sites of the array implanted in left area LIP for monkeys B (left) and W (right). Each circle corresponds to an electrode channel within the array. Red circles indicate sites that elicited saccades upon microstimulation. Blue circles designate sites that elicited blinks while white ones indicate sites in which no specific response was observed as a result of microstimulation. (B) Mapping the distribution of saccade onset thresholds using gradients of red. Circles with a cross sign refer to sites whose microstimulation did not evoke saccades. Dark red circles are sites with the highest saccade onset thresholds of above 200 μA. Light red marks sites with thresholds in the range of 150 to 200 μA. Orange marks sites with thresholds of 100 to 150 μA and light yellow indicates sites with the lowest saccade thresholds in the range of 40 to 100 μA. A: anterior, P: posterior, M: medial, L: lateral.

Figure 3. (A) Examples of saccades from a representative site (shown on bottom right) of the array that was microstimulated at three different current amplitudes: 75 μA (left), 100 μA (middle), 200 μA (right). For each plot, the dashed line marks the onset of microstimulation and the horizonal axis represents time in milliseconds with a calibration bar that represents 40 ms. The traces at the top refer to the horizontal eye movements (E_h), while the bottom ones refer to the vertical eye

movements (E_v). The calibration bar for the amplitude of these traces is given at 5 degrees for all plots. (B) Bar plot representing the percentage of saccades (vertical axis) elicited at each microstimulation current amplitude (horizontal axis) from the same representative site.

Figure 4. (A) Bar plot representing saccade onset latency from all saccadic sites of the array for both monkeys as a function of the amplitude of the microstimulation current. (B) Bar plot representing the duration of all saccades for both animals as a function of the amplitude of the microstimulation current. Error bars represent the standard deviation from the mean.

Figure 5. Representative examples of staircase saccades from two individual sites of the array, stimulated at 150 μA (left) and 225 μA (right) respectively. Dashed line refers to the onset of stimulation and the solid horizontal bar shows the duration of stimulation. The horizontal axis refers to time with a calibration bar of 40 ms. The traces on the top display horizontal eye movements (E_h) while the bottom traces show vertical eye movements (E_v), both with an amplitude calibration bar of 5 degrees.

Figure 6. (A) Mapping the average saccade vectors across all saccadic sites of the array for both monkeys B (left) and W (right). Each square corresponds to an array electrode. Grey squares refer to sites that did not elicit saccades upon microstimulation. Each arrow represents the average saccade vector evoked across all saccade trials, with its associated amplitude and direction. The amplitude of the saccades is measured by the calibration bar given for 2 degrees. Each arrow is plotted based on vertical and horizontal axes that represent vertical (E_v) and horizonal (E_h) eye movements, respectively. (B) Examples of individual saccades constituting an average saccade vector from four representative array sites per animal, marked by numbers 1, 2, 3, and 4 in (A). Saccade amplitude calibration bar is given for 2 degrees. Circles reflect the starting position of saccades. For each site, vertical and horizontal axes refer to vertical (E_v) and horizontal (E_h) eye movements, respectively. A: anterior, P: posterior, M: medial, L: lateral.

Figure 7. Effect of initial eye position on stimulation-evoked saccades. (A) Examples of the effect of initial eye position on evoked saccades from 2 representative sites of the array as marked on the array grid. Left: fixed-vector saccades, right: goal-directed saccades. Circles indicate the starting

position of saccades. Vertical and horizontal axes illustrate the distribution of starting position of saccades across the display. L: left, R: right, U: up, D: down. (B) Corresponding regression plots for the representative sites displayed on part A. Each figure displays two scatter plots for each of the horizontal (K_h, blue) and vertical (K_v, red) saccade components, with the vertical axis being the size of saccades defined as the difference of saccade offset and onset (ΔE_h: horizontal, ΔE_v: vertical), versus different initial eye positions (E_h: horizontal, E_v: vertical). Dots represent all saccade trials from that representative site and the line represents the regression line of best fit.

Figure 8. Bar plot representing the results of regression analysis from all the 10 sites of the array in which the effect of initial eye position was examined. These specific sites are marked on the array grid as shown on the top right of the figure. Left: bar plots representing slopes of horizontal saccade components, right: bar plots representing slopes of vertical saccade components. Horizontal axis represents individual sites and vertical axis represents slopes (left: horizontal, right: vertical).

References

Andersen RA, Asanuma C, Cowan WM. (1985) Callosal and prefrontal associational projecting cell populations in area 7a of the macaque monkey: A study using retrogradely transported fluorescent dyes. J Comp Neurol 232: 443-455.

Bruce CJ, Goldberg ME (1985) Primate frontal eye fields. I. single neurons discharging before saccades. J Neurophysiol 53:603–635.

Bakola S, Burman KJ, Rosa MGP (2015) The cortical motor system of the marmoset monkey (Callithrix jacchus). Neuroscience Research 93:72-81.

Belmonte JCI, Callaway EM, Caddick SJ, Churchland P, Feng G, Homanics GE, Lee KF, Leopold DA, Miller CT, Mitchell JF, Mitalipov S, Moutri AR, Movshon JA, Okano H, Reynolds JH, Ringach DL, Sejnowski TJ, Silva AC, Strick PF, Wu J, Zhang F (2015) Brains, Genes, and Primates. Neuron 986:617-631.

Blatt GJ, Andersen RA, Stoner GR (1990) Visual receptive field organization and cortico-cortical connections of the lateral intraparietal area (Area LIP) in the macaque. J Comp Neurol 299:421-445.

Bock NA, Kocharyan A, Liu JV, Silva AC (2009) Visualizing the entire cortical myelination pattern in marmosets with magnetic resonance imaging. J Neurosci Meth 185:15-22.

Burman KJ, Palmer SM, Gamberini M, Rosa MGP (2006) Cytoarchitectonic subdivisions of the dorsolateral frontal cortex of the marmoset monkey (Callithrix jacchus), and their projections to dorsal visual areas. J Comp Neurol 495:149-172.

Burman KJ, Palmer SM, Gamberini M, Spitzer MW, Rosa MGP (2008) Anatomical and physiologcial defninition of the motor cortex of the marmoset monkey. J Comp Neurol 506:860-876.

Chen CY, Matrov D, Ho KT, Isa T (2019) Topographic representation of saccade vector in frontal eye field of common marmoset. Society for the Neural Control of Movement Abstracts: 2A1.

Clark KL, Armstrong KM, Moore T (2011) Probing neural circuitry and function with electrical microstimulation. Proc R Soc B 278:1121-1130.

Collins CE, Lyon DC, Kaas JH (2005) Distribution across cortical areas of neurons projecting to the superior colliculus in new world monkeys. Anat Rec A Discov Mol Cell Evol Biol

285:619–627 Available at: http://www.ncbi.nlm.nih.gov/pubmed/15912524.

Cooke DF, Taylor CSR, Moore T, Graziano MSA (2003) Complex movements evoked by microstimulation of the ventral intraparietal area. Proc Nat Acad Sci USA 100:6163-6168.

Fleming JFR, Crosby EC (1955) The parietal lobe as an additonal motor area. The motor effects of electrical stimulation and ablation of cortical areas 5 and 7 in monkeys. J Comp Neurol 103:485-512.

French JA (2019) The marmoset as a model in behavioral neuroscience and psychiatric research. In: The Common Marmoset in Captivity and Biomedical Research. Elsevier, Amsterdam.

Ghahremani M, Hutchison RM, Menon RS, Everling S (2017) Frontoparietal Functional Connectivity in the Common Marmoset. Cereb Cortex:1–16.

Hanes DP, Wurtz RH (2001) Interaction of the frontal eye field and superior colliculus for saccade generation. J Neurophysiol 85:804–815.

Heiney SA, Blazquez PM (2011) Behavioral response of trained squirred and rhesus monkeys during oculomotor tasks. Exp Brain Res 212:409-416.

Johnston K, Everling S (2008) Neurophysiology and neuroanatomy of reflexive and voluntary saccades in non-human primates. Brain Cogn 68:271–283.

Johnston KD, Barker K, Schaeffer L, Schaeffer DJ, Everling S (2018) Methods for chair restraint and training of the common marmoset on oculomotor tasks. J Neurophysiol. 119:1636-1646.

Kaas JH (19897) The organization of neocortex in mammals: Implications for theories of brain function. 38:129-151.

Kelly RC, Smith MA, Samonds JM, Kohn A, Bonds AB, Movshon JA, Sing Lee T (2007) Comparison of Recordings from Microelectrode Arrays and Single Electrodes in the Visual Cortex. J Neurosci 27:261–264.

Krubitzer L (1995) The organization of neocortex in mammals: are species differences really so different. Trends Neurosci 18:408-417.

Kurylo DD, Skavenski a a (1991) Eye movements elicited by electrical stimulation of area PG in the monkey. J Neurophysiol:1243–1253.

Liu C, Ye FQ, Yen CCC, Newman JD, Glen D, Leopold DA, Silva AC (2018) A digital 3D atlas of the marmoset brain based on multi-modal MRI. Neuroimage 169:106–116.

Lu T, Liang L, Wang X (2001) Neural representations of temporally asymmetric stimuli in the

auditory cortex of awake primates. J Neurophysiol 85:2364–2380.

Lynch JC, Graybiel AM, Lobeck LJ (1985). The differential projection of two cytoarchitectonic subregions of the inferior parietal lobule of macaque upon the deep layers of the superior colliculus. J Comp Neurol 235:241-254.

Mansfield K (2003) Marmoset models commonly used in biomedical research. Comp Med 53:838-392.

Mitchell JF, Leopold DA (2015) The marmoset monkey as a model for visual neuroscience. Neurosci Res 93:20–46

Mitchell JF, Reynolds JH, Miller CT (2014) Active vision in marmosets: A model system for visual neuroscience. J Neurosci 34: 1183-1194.

Newman JD, Kenkel WM, Aronoff EC, Bock NA, Zametkin MR, Silva AC (2009) A combined histological and MRI brain atlas of the common marmoset monkey, Callithrix jacchus. Brain Res Rev 62:1–18.

Nicolelis MAL, Dimitrov D, Carmena JM, Crist R, Lehew G, Kralik JD, Wise SP (2003) Chronic, multisite, multielectrode recordings in macaque monkeys. Proc Natl Acad Sci 100:11041–11046.

Normann RA, Fernandez E (2016) Clinical applications of penetrating neural interfaces and Utah Electrode Array technologies. J Neural Eng:1–16.

Nudo RJ, Sutherland DP, Masterton RB (1995) Variation and evolution of mammalian corticospinal somata with special reference to primates. J Comp Neurol 358:181-205.

Okano H, Mitra P (2015) Brain-mapping projects using the common marmoset. Neuroscience Research 93:3-7.

Okano H, Sasaki E, Yamamori T, Iriki A, Shimogori T, Yamaguchi Y, Kasai K, Miyawaki A (2016) Brain/MINDS: A Japanese National Brain Project for Marmoset Neuroscience. Neuron:582–590.

Paxinos G, Watson C, Petrides M, Rosa MGP, Tokuno H (2012) The marmoset brain in stereotaxic coordinates. San Diego: Elsevier Academic Press.

Reser DH, Burman KJ, Yu HH, Chaplin TA, Richardson KE, Worthy KJ, Rosa MGP (2013). Contrasting patterns of cortical input to architectural subdivisions of the area 8 complex: A retrograde tracing study in marmoset monkeys. Cereb Cortex 23:1901-1922.

Rosa MGP, Palmer SM, Gamberini M, Burman KJ, Yu HH, Reser DH, Bourne JA, Tweedale R,

Galetti C (2009). Connections of the dorsomedial visual area: Pathways for early integration of dorsal and ventral streams in extrastriate cortex. J Neurosci 29: 4548-4563.

Rosa MGP, Tweedale R (2000) Visual areas in lateral and ventral extrastriate cortices of the marmoset monkey. J Comp Neurol 422:621-651.

Russo GS, Bruce CJ (1993) Effect of eye position within the orbit on electrically elicited saccadic eye movements: a comparison of the macaque monkey's frontal and supplementary eye fields. J Neurophysiol 69:800–818.

Schiller PH, Tehovnik EJ (2001) Look and see: how the brain moves your eyes about. Prog Brain Res 134:127-142.

Selemon LD, Goldman Rakic PS (1988) Common cortical and subcortical targets of the dorsolateral prefrontal and posterior parietal cortices in the rhesus monkey: evidence for a distributed neural network subserving spatially guided behavior. J Neurosci 8:4049-4068.

Selvanayagam J, Schaeffer L, Johnston K, Everling S (2019) Identification of the frontal eye fields in the common marmoset using microstimulation. Society for the Neural Control of Movement Abstracts: 2A5.

Shibutani H, Sakata H, Hyvärinen J (1984) Saccade and blinking evoked by microstimulation of the posterior parietal association cortex of the monkey. Exp Brain Res 55:1–8.

Solomon SS, Tailby C, Ghareai S, Camp AJ, Bourne JA, Solomon SG (2011) Visual motion integration by neurons in the middle temporal area of a New World monkey, the marmoset. J Physiol 589: 5741-5758.

Solomon SG, Rosa MGP (2014) A simpler primate brain: the visual system of the marmoset monkey. Front Neural Circuits 8:96.

Thier P, Andersen RA (1996) Electrical microstimulation suggests two different forms of representation of head-centered space in the intraparietal sulcus of rhesus monkeys. Proc. Nat. Acad. Sci. USA 93:4962-4967.

Thier P, Andersen RA (1998) Electrical Microstimulation Distinguishes Distinct Saccade-Related Areas in the Posterior Parietal Cortex. J Neurophysiol:1713–1735.

Tomlinson RD, Bahra PS (1986) Combined eye-head gaze shifts in the primate. I. Metrics. J Neurophysiol 56:1542-1557.

Van Essen DC, Drury H a., Dickson J, Harwell J, Hanlon D, Anderson CH (2001) An integrated software suite for surface-based analyses of cerebral cortex. J Am Med Informatics Assoc

8:443–459.

Wang X, Lu T, Snider RK, Liang L (2005) Sustained firing in auditory cortex evoked by preferred stimuli. Nature 435:341–346.

Wurtz R, Goldberg M (1989) The neurobiology of saccadic eye movements. (Wurtz R, Goldberg M, eds)., illustrate. Elsevier.

Wurtz RH, Goldberg ME (1971) Superior colliculus cell responses related to eye movements in awake monkeys. Science (80-) 171:82–84.

Figures:

Figure 1.

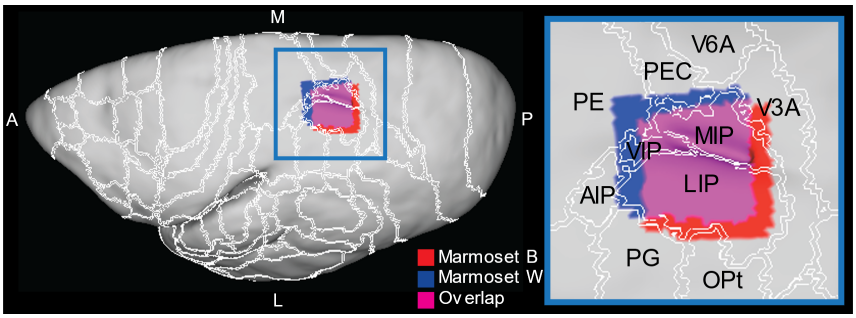

Figure 2.

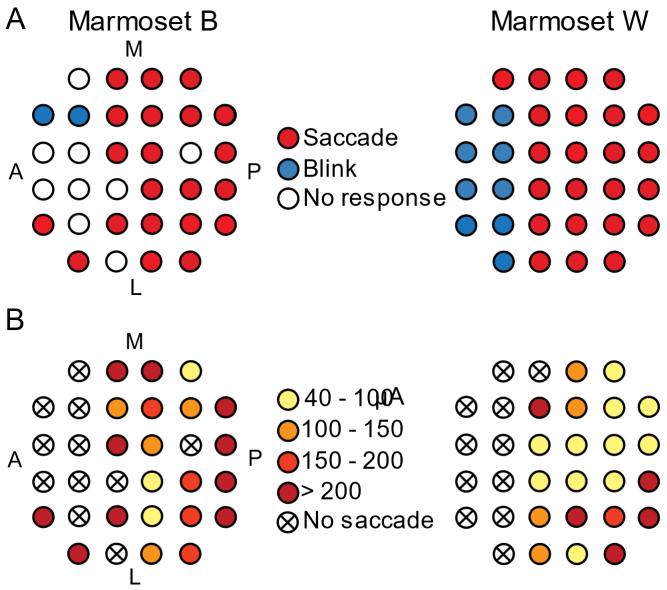
A
Marmoset B
Marmoset W
M
A
P
L
Saccade
Blink
No response
B
M
A
P
L
40 - 100
100 - 150
150 - 200
> 200
No saccade

Figure 3.

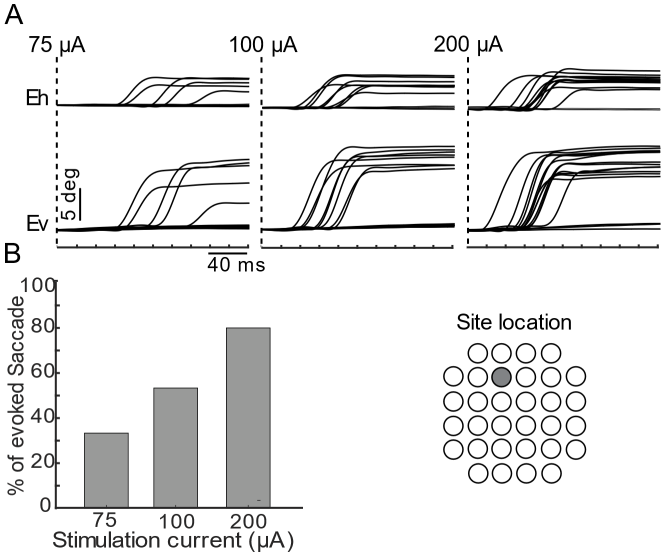
A
75 μA
100 μA
200 μA
Eh
Ev
5 deg
40 ms
B
% of evoked Saccade
100
80
60
40
20
0
75
100
200
Stimulation current (μA)
Site location

Figure 4.

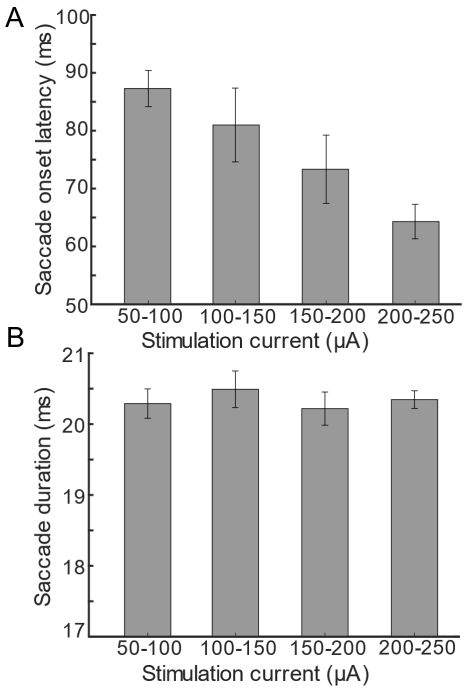
A
Saccade onset latency (ms)
100
90
80
70
60
50
50-100
100-150
150-200
200-250
Stimulation current (μA)
B
Saccade duration (ms)
21
20
19
18
17
50-100
100-150
150-200
200-250
Stimulation current (μA)

Figure 5.

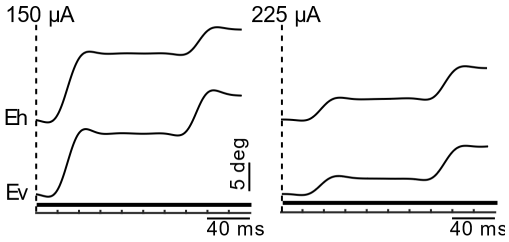

Figure 6.

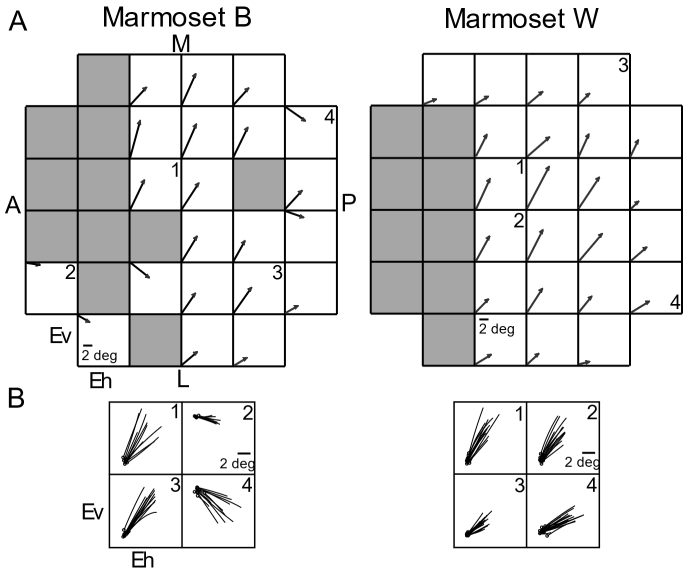

Figure 7.

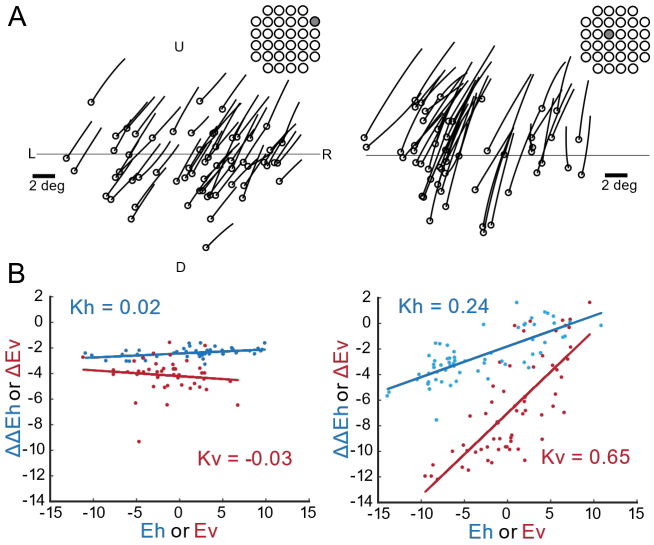
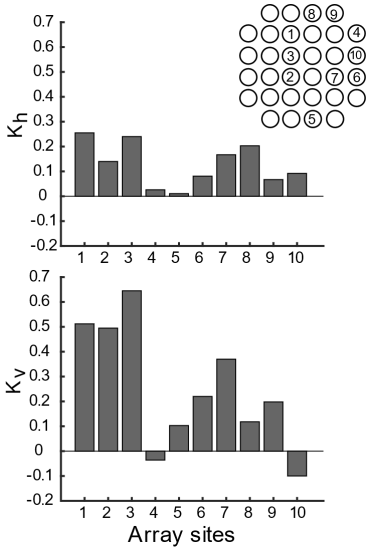
Figure 8.